Korean J. Chem. Eng., 36(7), 1042-1050 (2019)
DOI: 10.1007/s11814-019-0281-3

pISSN: 0256-1115
eISSN: 1975-7220

Optimization of fructose dehydration to 5-hydroxymethylfurfural catalyzed by SO_3H-bearing lignin-derived ordered mesoporous carbon

Shuai Wang, Li Lyu, Guobao Sima, Ying Cui, Baoxia Li, Xueqin Zhang, and Linhuo Gan†

College of Chemical Engineering, Huaqiao University, Xiamen, 361021, Fujian, China
(*Received 29 January 2019 • accepted 23 April 2019*)

Abstract−A sulfonated lignin-derived mesoporous carbon (LDMC-SO_3H) was prepared from kraft lignin (KL) using phenolation and soft-template method followed by sulfonation. LDMC-SO_3H bearing a sulfonic acid density of 0.65 mmol/g possessed a well-ordered 2D hexagonal mesoporous characteristics with mesopore volume of 0.067 cm^3/g and specific surface area of 262 m^2/g as well as mesopore size of 3.42 nm. A high 5-hydroxymethylfurfural (5-HMF) yield of 98.0% with a full fructose conversion was obtained using LDMC-SO_3H as catalyst under the optimized reaction conditions of reaction temperature and time of 140 °C and 120 min, initial fructose concentration of 100 g/L, catalyst load of 0.1 mg/mg in DMSO. Furthermore, there was no obvious decrease in 5-HMF yield (≥95.0%) within the five-cycle experiment, highlighting the superior reusability and stability of LDMC-SO_3H in fructose-to-5-HMF transformation.

Keywords: Kraft Lignin, Soft-template Method, Ordered Mesoporous Carbon, Solid Acid, 5-Hydroxymethylfurfural

INTRODUCTION

The current research hotspot of biomass energy is to synthesize biomass-derived platform compounds from carbohydrates. Among them, 5-hydroxymethylfurfural (5-HMF) is a significant biomass-derived green platform compound possessing highly reactive sub-structures including furan ring, hydroxymethyl group and aromatic aldehyde [1], which can be prepared from acid-catalyzed dehydration of renewable biomass feedstocks [2,3]. In the past few years, various biomasses have been used as raw materials to prepare 5-HMF via dehydration, in which the dehydration of fructose by acidic catalysis is the most effective route (Scheme 1).

Catalysts commonly used in the dehydration of fructose are mainly liquid acids such as HCl [4] and H_2SO_4 [5], which exhibit good catalytic efficiency. However, the application of solid acids in this field has gradually attracted widespread attention [6], mainly because solid acids overcome some of the serious challenges faced by liquid acids such as strong corrosion, high toxicity and poor recyclability [7,8]. Most importantly, the effectiveness in the dehydration of fructose to 5-HMF is more closely related to structural characteristics

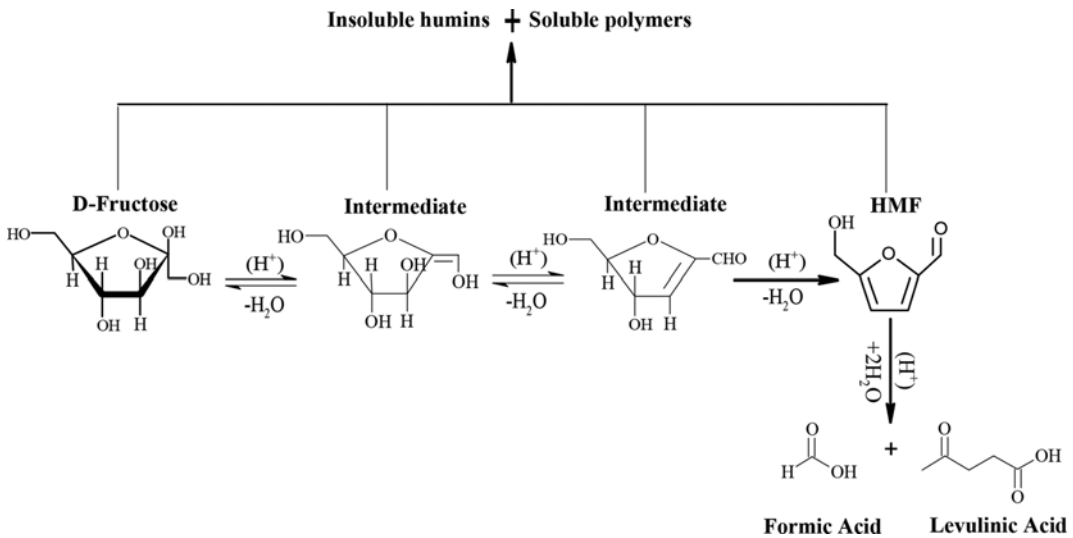

Scheme 1. Schematic illustration of fructose dehydration into HMF [2].

†To whom correspondence should be addressed.
E-mail: lhgan401@126.com

Table 1. Dehydration of fructose to 5-HMF with water or/and DMSO as solvent

Catalyst	Solvent	Fructose conversion (%)	5-HMF yield (%)
Amberlyst-70 [12]	Water	80.1	45.6
Glu-TsOH [13]	Water	67.0	8.0
PSSH-grafted particle [14]	Water	80.0	27.0
HSO_3-fiber [15]	Water	72.0	34.0
H_2PO_3-fiber [15]	Water	79.0	27.0
SiNP-SO_3H-C_{16} [16]	Water/DMSO	100.0	87.0
Glu-TsOH [13]	DMSO	99.9	91.2
HPW/MCM [17]	DMSO	100.0	80.0
MLC-SO_3H [18]	DMSO	100.0	81.1
OMC-SO_3H [19]	DMSO	98.7	89.4
CS-2 [20]	DMSO	100.0	90.0
LDMC-SO_3H[a]	DMSO	100.0	98.0

[a]LDMC-SO_3H is the catalyst prepared in this work

of solid acids and reaction solvent. On one hand, acid sites on solid catalysts undoubtedly play a key role in the dehydration reaction of fructose to 5-HMF, but other factors including the acid sites accessibility can affect the catalytic performance of solid acids when the density of acidic groups reaches a certain value [9]. On the other hand, water is absolutely a green sustainable solvent, but it is not ideal for converting fructose into 5-HMF due to the formation of by-products in aqueous system [10]. Thus, organic solvents are commonly used as reaction medium, such as DMSO, which can shorten reaction time and suppress side reactions significantly [11]. Table 1 lists the research results of the preparation of 5-HMF via fructose conversion using water or DMSO as solvent in recent years.

Currently, ordered mesoporous carbon (OMC) has been widely used as a catalyst carrier due to its remarkable properties such as mesoporous structure, high surface area and good chemical stability. Although OMC has long been synthesized by hard-template method, soft-template method has become more and more popular owing to several difficulties associated with the hard-template method such as the use of toxic and corrosive chemicals. Recently, the acid-functionalized OMC prepared by soft-template method has been employed in the production of 5-HMF via fructose dehydration with good catalytic performance [19,21]. However, most of carbon sources currently used for preparing OMC are petrochemical materials such as phenol [22] and resorcinol [23], which increases the preparation cost and contains certain toxicity. As is known, lignin is a kind of natural biopolymer consisting of plenty of aromatic rings or phenolic hydroxyl groups, which can be employed as a promising natural substitute for phenol to crosslink with formaldehyde to synthesize phenol formaldehyde resin [24]. However, the highly branched structure of lignin makes it difficult to produce highly controlled porosity and ordered structures. Phenolation has been adopted widely to improve the solubility and reac-

Scheme 2. Schematic illustration of the synthesis process of sulfonated lignin-derived ordered mesoporous carbon derived from kraft lignin.

tivity of lignin, which makes it more suitable for the synthesis of lignin-phenol-formaldehyde (LPF) resin [25,26].

In this work, OMC was prepared successfully using soft-template method and kraft lignin (KL) as carbon resource, and the corresponding sulfonated product was obtained by sulfonation. The specific process diagram is shown in Scheme 2. Herein, we creatively used a liquefied KL degradation product to crosslink with formaldehyde to form phenolic resin as carbon precursor for the synthesis of lignin-derived mesoporous carbon (LDMC). Sulfonic acid-functionalized lignin-derived ordered mesoporous carbon (LDMC-SO_3H) was then prepared via sulfonation in concentrated sulfuric acid. And the structure of the optimized LDMC-SO_3H catalyst was characterized in detail. Furthermore, the effects of reaction temperature and time, initial fructose concentration, catalyst load (mass ratio of catalyst to fructose) and volume ratio of water to DMSO on the conversion of fructose into 5-HMF were investigated, respectively. Finally, the stability of as-prepared LDMC-SO_3H was studied under the optimized conditions.

EXPERIMENTAL

1. Materials

Kraft lignin and Pluronic F127 ($EO_{106}PO_{70}EO_{106}$, Mw=12,600) were obtained from Sigma-Aldrich Corporation. Formaldehyde solution (HCHO, 37-40%), phenol (C_6H_5OH, >99.8%), hydrochloric acid (HCl, 36-38%), sulfuric acid (H_2SO_4, 95-98%), sodium hydroxide (NaOH, >96%), ethanol (C_2H_5OH, >99.7%), dimethyl sulfoxide (DMSO, >99.5%) and fructose (>99%) were purchased from Xilong Chemical Co., Ltd., China. 5-hydroxymethylfurfural (5-HMF, >95%) and 5-hydroxymethylfurfural (5-HMF, HPLC solvent) were obtained from Aladdin Industrial Inc.

2. Preparations of LDMC and LDMC-SO_3H

2.0 g of kraft lignin, 0.4 g of NaOH, 6.0 g of water and 6.0 mL of phenol were mixed and transferred to a 150 mL of three-necked flask, then the mixture was stirred and heated in an oil bath for 2 h at 160 °C. After the solution was cooled to room temperature quickly, ethanol solution (10 mL, 50 wt%) and formaldehyde solution (16 mL, 37%) were added and stirred at 70 °C for 12 h. Next, hydrochloric acid (2.0 mol/L) was used to adjust the pH of reaction system to 7.0. Afterward, the LPF solution was obtained after removing solvent using rotary evaporation, and then was dissolved in ethanol to remove the precipitated salt. At the same time, 14 g of Pluronic F127 was dissolved in 225 mL of ethanol in a magnetic stirring manner at 40 °C to get a surfactant solution. Next, LPF solution and surfactant solution were uniformly mixed and stirred for 12 h, then volatilized at room temperature for 8 h and thermo-polymerized for 24 h at 100 °C in an oven and then placed in a tube furnace followed by carbonization at 900 °C for 3 h under the condition of nitrogen atmosphere to obtain LDMC.

The obtained LDMC and concentrated sulfuric acid (98%) were added to an autoclave at a certain mass & volume ratio (w/v, 1 : 20) and uniformly mixed, followed by reaction for 12 h at 180 °C under nitrogen atmosphere. And then it was washed repeatedly by hot water (>80 °C) until sulfate ions were not detected in the filtrate. The sulfonated product was placed in an oven and dried for 8 h at 60 °C to get the LDMC-SO_3H.

3. Characterization

Fourier transform infrared spectroscopy (FTIR) spectrum of LDMC-SO_3H was recorded on a Nicolet iS50 FTIR infrared spectrometer over the scanning range from 400 to 4,000 cm^{-1}. The small-angle X-ray scattering (SAXS) pattern of LDMC-SO_3H was performed on a Rigaku Smart Lab type X-ray diffractometer using Cu Kα as radiation source operated at 40 mA and 40 kV with a scanning speed of 1° per min in a 2θ range from 0.6 to 5°. N_2 adsorption-desorption isotherm was measured using an ASAP 2020 gas adsorption analyzer at 77.35 K. Transmission electron microscopy (TEM) image of LDMC-SO_3H was obtained using an FEI Tecnai G2 F20 200 kV field emission transmission electron microscope. Temperature programmed desorption using NH_3 as adsorbate (NH_3-TPD) curve of LDMC-SO_3H was determined by a ChemiSorb 2720 automatic chemisorption instrument with helium as carrier at 40 mL/min of flow rate. X-ray diffraction (XRD) pattern of LDMC-SO_3H was performed on a Rigaku Smart Lab X-ray diffractometer with Cu Kα radiation at 40 kV and 30 mA in a 2θ range from 10 to 80° with a scanning speed of 4° per min. The TGA spectrum of LDMC-SO_3H was measured by Shimadzu DTG-60H thermal analyzer under argon atmosphere with a temperature range from 20 to 900 °C at a heating rate of 10 °C per min.

The content of sulfonic acid (-SO_3H) group (mmol/g) is determined by the acid-base back titration method performed on a WDDY-2008J microcomputer automatic potentiometric titrator (China). First, a certain amount of LDMC-SO_3H was added to 20 mL of NaCl aqueous solution (2.0 mol/L), shaken at room temperature for 12 h, and then filtered. The filtrate was titrated by NaOH standard solution (0.01 mol/L). As a result, the loading amount of -SO_3H group was calculated to be 0.65 mmol/g.

4. Fructose Conversion into 5-HMF

Fructose, LDMC-SO_3H and DMSO were added to a 25 mL digestion tube. The mixture was purged by nitrogen for 2 min and shaken vigorously (200 rpm) in a shaking table. Subsequently, the reaction system reacted at the desired reaction temperature for a certain period of time. Then the suspension was filtered using a 0.22 μm filter, and the concentrations of fructose and 5-HMF in the filtrate were measured using high performance liquid chromatography (HPLC). In the recycling experiments, LDMC-SO_3H was isolated from the reaction system via centrifugation, then washed with ethanol three times and dried overnight at 80 °C for the next run under the same reaction conditions.

5. Analysis of Product

The concentration of 5-HMF was measured using an HPLC apparatus (Elite P-1201, Dalian, China) fitted with an Agilent ZORBAX Eclipse Plus C18 column (Ø4.6×250 mm) and a UV-Vis detector (λ=284 nm). The mixture solution of water and methanol (4/1, v/v) is the mobile phase with a certain flow rate (0.8 mL/min) at column temperature of 50 °C. The measurement of fructose concentration was performed on an HPLC apparatus (Agilent 1260 Infinity II) equipped with an Agilent ZORBAX carbohydrate analysis column (Ø4.6×250 mm) and a refractive index detector. The mixture solution of water and acetonitrile (1/3, v/v) is the mobile phase with a certain flow rate (1.0 mL/min) at column temperature of 50 °C. Thus, conversion of fructose (X), yield of 5-HMF (Y) and reaction selectivity (S) were determined by the following Eqs. (1)-(3), respectively.

$$X(\%)=\left(1-\frac{\text{Mole concentration of fructose in product}}{\text{Mole concentration of initial fructose}}\right)\times 100\% \quad (1)$$

$$Y(\%)=\left(\frac{\text{Mole concentration of 5-HMF produced}}{\text{Mole concentration of initial fructose}}\right)\times 100\% \quad (2)$$

$$S(\%)=\left(\frac{\text{5-HMF yield}}{\text{Fructose conversion}}\right)\times 100\% \quad (3)$$

RESULTS AND DISCUSSION

1. Characterization

Fig. 1 shows the XRD pattern of LDMC-SO_3H catalyst. Two characteristic peaks appear at 2θ=23° and 43°, which are attributed to (002) and (100) diffraction, respectively. The result shows that the as-prepared catalyst has a certain degree of graphite structure via the carbonization process of LDMC at 900 °C, which provides a relatively stable structure for the sulfonation treatment of LDMC at 180 °C and the utilization of LDMC-SO_3H in catalytic reaction of fructose conversion into 5-HMF at higher than 100 °C.

Fig. 2 indicates the FTIR spectrum of LDMC-SO_3H catalyst. As seen in Fig. 2, the peak at 3,430 cm^{-1} can be attributed to O-H stretching vibration in -OH groups [27-29]. More importantly, the peaks at 1,384 cm^{-1} and 1,084 cm^{-1} are related to O=S=O stretching vibration in -SO_3H groups [29-31], and the peak at 804 cm^{-1} is related to C-O-S stretching vibration [32], thus indicating that -SO_3H groups are successfully incorporated into the structure of LDMC. Most importantly, because the hydrophobic nature of 5-HMF is more than that of fructose, it is suggested that the interface with a certain hydrophilic degree originated from the hydrophilic functional groups of -SO_3H groups and -OH groups in LDMC-SO_3H structure, can facilitate the adsorption of fructose onto LDMC-SO_3H for contacting with its catalytic active sites (-SO_3H groups) to increase fructose conversion and the rapid detachment of reaction product (5-HMF) from catalyst (LDMC-SO_3H) to enhance 5-HMF yield and reaction selectivity [33].

Fig. 3 shows the SAXS curve of LDMC-SO_3H. In Fig. 3, LDMC-SO_3H exhibits an intense diffraction peak at around 1°, which can be indexed as (100) reflection associated with hexagonal pore regularity of the 2D *p6mm* space group [34], highlighting an ordered pore structure of LDMC-SO_3H.

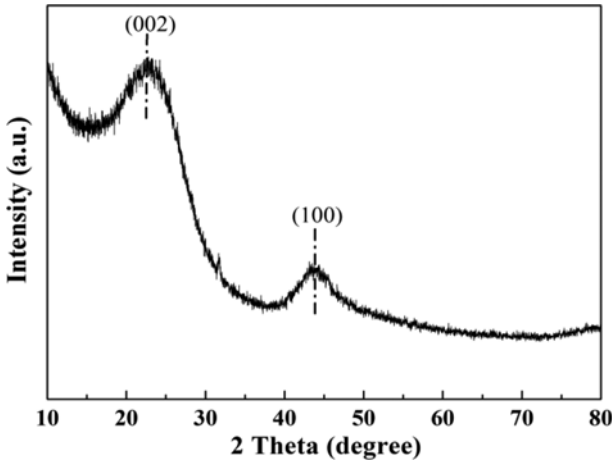

Fig. 1. XRD pattern of LDMC-SO_3H.

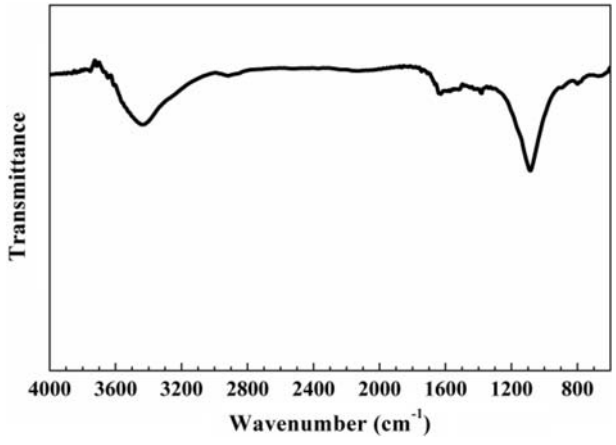

Fig. 2. FTIR spectrum of LDMC-SO_3H.

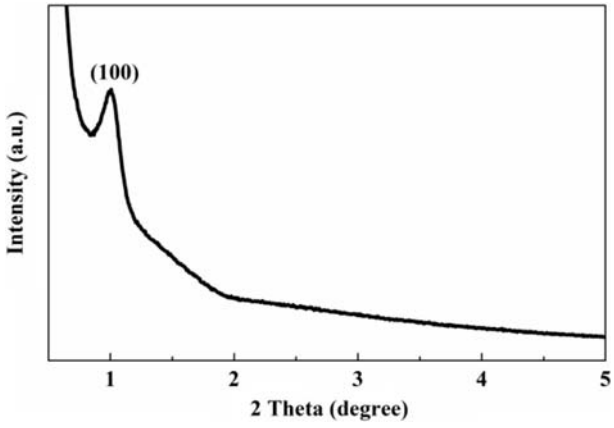

Fig. 3. SAXS curve of LDMC-SO_3H.

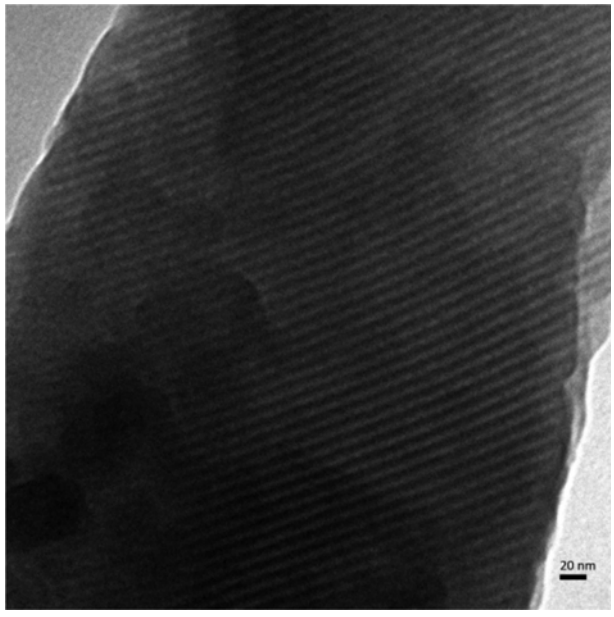

Fig. 4. TEM image of LDMC-SO_3H.

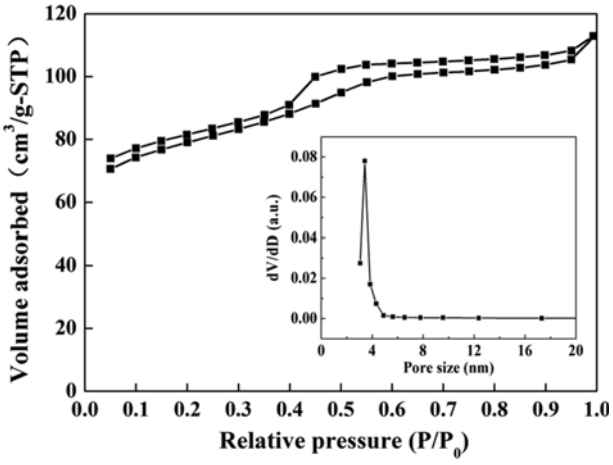

Fig. 5. Nitrogen adsorption-desorption isotherm and pore size distribution of LDMC-SO_3H.

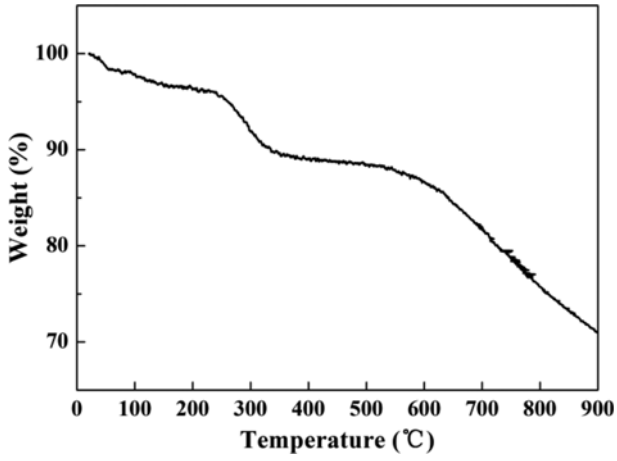

Fig. 7. TGA spectrum of LDMC-SO_3H.

Fig. 4 shows the TEM image of LDMC-SO_3H to investigate its morphology. As shown in Fig. 4, LDMC-SO_3H displays a mesoporous structure with stripe-like patterns in large part areas, confirming an ordered two-dimensional mesoporous characteristics.

Fig. 5 shows the nitrogen adsorption-desorption isotherm and pore size distribution of LDMC-SO_3H catalyst. As seen in Fig. 5, there is a type-IV curve with a hysteresis loop in the relative pressure at P/P_0=0.4-0.6, reflecting high uniformity of mesoporous structure [35,36]. The pore size distribution is computed from branch of the adsorption-desorption isotherm using the BJH method, and the mesopore diameter of LDMC-SO_3H is centered at about 3.42 nm. The mesopore volume and specific surface area are up to 0.067 cm^3/g and 262 m^2/g, respectively.

Fig. 6 shows the NH_3-TPD profile of LDMC-SO_3H catalyst. Acid sites can be classified as weak (≤200 °C), medium (200-500 °C), and strong (≥500 °C) strength according to NH_3 desorption temperature, respectively [37]. The NH_3-TPD profile of LDMC-SO_3H shows that three NH_3 desorption peaks are detected in a tested temperature range from 50 to 800 °C, belonging to three different acid sites, respectively. The result shows that the as-prepared LDMC-SO_3H catalyst has two weak peaks at around 100 °C and 660 °C belonging to weak acid sites and strong acid sites, respectively. Notably, there is an intense peak at around 280 °C belonging to medium acid sites.

Fig. 7 shows the TGA spectrum of LDMC-SO_3H catalyst. As seen in Fig. 7, LDMC-SO_3H is relatively stable below 230 °C, although it has a slight loss in weight, which can be attributed to the evaporation of adsorbed water in LDMC-SO_3H. In the temperature range from 230 to 350 °C, the weight of LDMC-SO_3H decreases sharply, which can be attributed to the decomposition of the -SO_3H groups [38]. When the temperature is higher than 350 °C, the weight of LDMC-SO_3H will decrease slowly and continuously, which can be attributed to further condensation of amorphous carbon.

2. Optimization of Fructose Dehydration to 5-HMF

2-1. Effects of Reaction Time and Temperature

The effects of reaction time and temperature on fructose conversion, 5-HMF yield and reaction selectivity were studied, and the results are shown in Fig. 8 and Fig. 9, respectively. As shown in

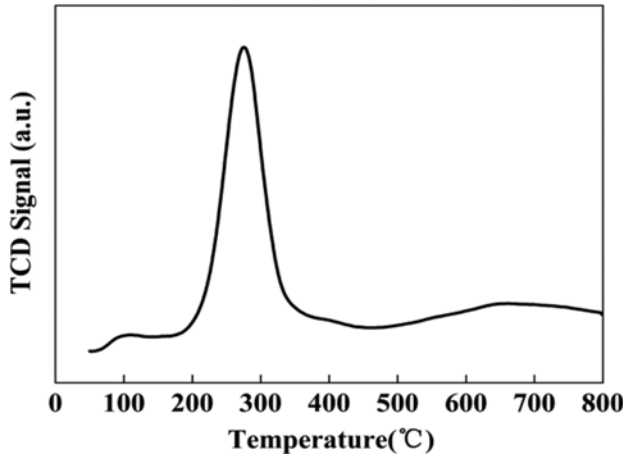

Fig. 6. NH_3-TPD curve of LDMC-SO_3H.

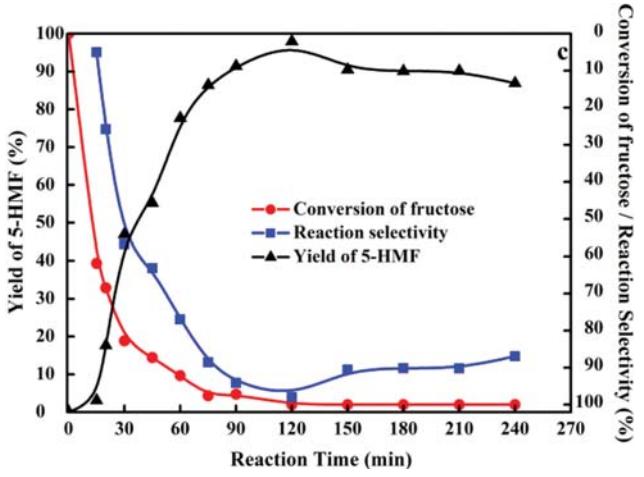

Fig. 8. Changes of fructose conversion, 5-HMF yield and reaction selectivity with reaction time. Reaction condition: reaction temperature of 140 °C, initial fructose concentration of 100 g/L, catalyst load of 0.1 mg/mg, solvent of DMSO.

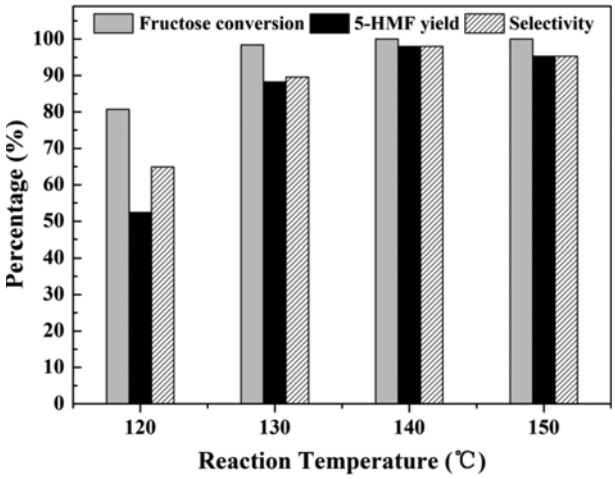

Fig. 9. Changes of fructose conversion, 5-HMF yield and reaction selectivity with reaction temperature. Reaction condition: reaction time of 120 min, initial fructose concentration of 100 g/L, catalyst load of 0.1 mg/mg, solvent of DMSO.

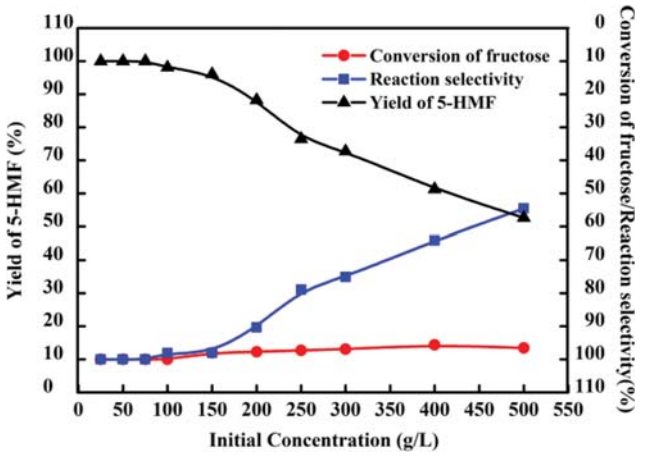

Fig. 10. Effect of initial fructose concentration on fructose conversion, 5-HMF yield and reaction selectivity. Reaction condition: reaction temperature and time of 140 °C and 120 min, catalyst load of 0.1 mg/mg, solvent of DMSO.

Fig. 8, fructose conversion enhances with prolonging reaction time until it reaches a high equilibrium value or fructose is even transformed completely. As reaction time increases to 120 min, fructose conversion, 5-HMF yield and reaction selectivity gradually increase to the maximum values of 100.0%, 98.0% and 98.0%, respectively. After 120 min, there are slight decreases in 5-HMF yield and reaction selectivity, mainly because 5-HMF can further react to form by-products as shown in Scheme 1. Seen from Fig. 9, when reaction temperature is 120 °C, fructose conversion, 5-HMF yield and reaction selectivity are only 80.7%, 52.4% and 64.9%, respectively. When reaction temperature increases from 120 °C to 140 °C, fructose conversion, 5-HMF yield and reaction selectivity obviously increase to 100.0%, 98.0% and 98.0%, respectively. With further increasing reaction temperature to 150 °C, 5-HMF yield and reaction selectivity decrease slightly to 95.3% and 95.3% probably due to an increase in the risk of generation of the by-products including soluble substances derived from rehydration of 5-HMF and insoluble humins. Within the scope of experimental conditions, fructose conversion, 5-HMF yield and reaction selectivity reach the maximum values of 100%, 98.0% and 98.0% when reaction temperature and time are 140 °C and 120 min, respectively.

2-2. Effect of Initial Fructose Concentration

During the dehydration of fructose to prepare 5-HMF catalyzed by acid, the initial concentration of fructose has non-negligible effects on 5-HMF yield and reaction selectivity [39]. The effect of initial substrate concentration on fructose conversion, 5-HMF yield and reaction selectivity at 140 °C in 120 min was investigated and the result is shown in Fig. 10.

As can be seen from Fig. 10, fructose is completely converted to 5-HMF and the value of 5-HMF yield is equal to reaction selectivity (98.0%) when initial fructose concentration is 100 g/L. With increasing substrate concentration, fructose conversion does not change significantly, but both 5-HMF yield and reaction selectivity decrease dramatically. In the experimental scope of initial fructose concentration, nearly all of fructose is converted into 5-HMF at 140 °C within 120 min when initial fructose concentration is not more than 100 g/L. However, with increasing initial fructose concentration to be higher than 100 g/L, the decrease in fructose conversion is much less than those in 5-HMF yield and reaction selectivity, indicating that more fructose is converted to other compounds but 5-HMF. More 5-HMF will be produced from fructose dehydration with increasing initial fructose concentration, which further accelerates the dehydration of 5-HMF to other substances with smaller molecular weight such as levulinic acid [40-42], thus resulting in the gradual decreases in 5-HMF yield and reaction selectivity. At the same time, a higher initial fructose concentration can increase the probability of collision between fructose molecules, leading to the formation of humins by self-polymerization or cross-polymerization [43-46]. Based on the above result, the optimal initial fructose concentration is determined to be 100 g/L at 140 °C for 120 min.

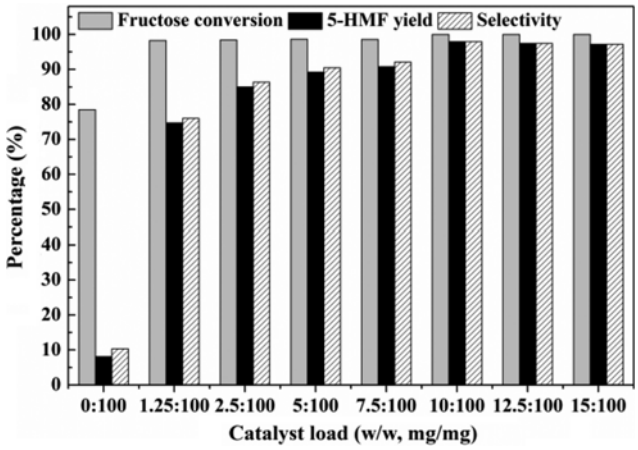

Fig. 11. Effect of catalyst load on fructose conversion, 5-HMF yield and reaction selectivity. Reaction condition: reaction temperature and time of 140 °C and 120 min, initial fructose concentration of 100 g/L, solvent of DMSO.

2-3. Effect of Catalyst Load

The effect of catalyst load on fructose conversion, 5-HMF yield and reaction selectivity was investigated and indicated in Fig. 11.

As can be seen from Fig. 11, fructose conversion, 5-HMF yield and reaction selectivity are very low (78.5%, 8.1% and 10.3%) in the absence of solid catalyst and then significantly improved with addition of LDMC-SO_3H catalyst, indicating that LDMC-SO_3H can accelerate the conversion of fructose to 5-HMF. However, the increases in 5-HMF yield and reaction selectivity far exceed that in fructose conversion. It is widely believed that the dehydration of fructose to 5-HMF catalyzed by an acid catalyst is via an open-chain or a cyclic furanose intermediate pathway [5]. Amarasekara et al. [47] determined a key intermediate generated by the dehydration of fructose to 5-HMF in DMSO at 150 °C without solid catalyst and found the synergistic catalysis between DMSO solvent and acid catalyst. In this work, it may spend longer time on dehydration reaction of fructose to form intermediates in DMSO when there is no solid catalyst, and LDMC-SO_3H can accelerate intermediate reactions and then produces a larger amount of 5-HMF for a certain reaction time. In the catalyst load range of 0.0-0.1 mg/mg, 5-HMF yield and reaction selectivity are enhanced gradually with increasing catalyst load, finally achieving the maximum values of 98.0% when catalyst load reaches 0.1 mg/mg (10 : 100, w/w). However, with further increasing catalyst dosage, there are no obvious variations in fructose conversion, 5-HMF yield and reaction selectivity, highlighting an availability of sufficient catalytic sites for fructose conversion to 5-HMF. In the summary, the optimum catalyst load is 0.1 mg/mg in this work.

2-4. Effect of Volume Ratio of Water to DMSO

In general, water plays a negative role in the dehydration of fructose to 5-HMF [39,43,48]. The effect of volume ratio of water to DMSO on fructose conversion, 5-HMF yield and reaction selectivity was investigated and the result is demonstrated in Fig. 12.

As shown in Fig. 12, 5-HMF yield and fructose conversion are only 1.7% and 15.7% in aqueous system, respectively. With increasing DMSO content in solvent system, fructose conversion, 5-HMF yield and reaction selectivity are gradually improved and reach the maximum values of 100.0%, 98.0%, 98.0% in pure DMSO, confirming that water can inhibit the dehydration reaction of fructose to prepare 5-HMF. It may be mainly because the reaction to produce 5-HMF from fructose is a dehydration reaction, which is not favorable in aqueous solution. Furthermore, 5-HMF will also rehydrate with water to form levulinic acid and formic acid. It has been reported that high 5-HMF yield and reaction selectivity are obtained in DMSO, in which the formation of by-products mentioned above can be inhibited to a large extent [2,49,50].

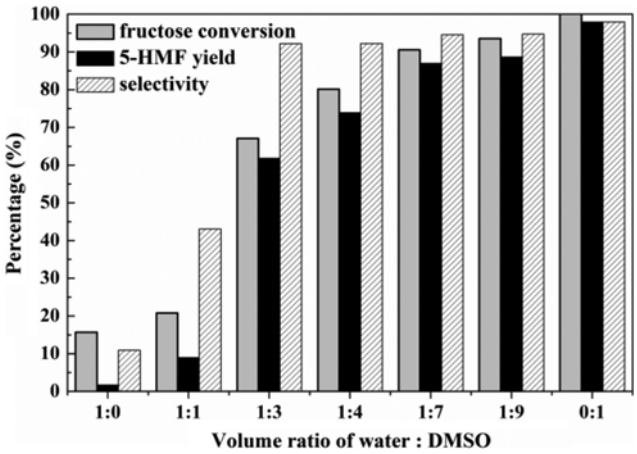

Fig. 12. Effect of volume ratio of water to DMSO on fructose conversion, 5-HMF yield and reaction selectivity. Reaction condition: reaction temperature and time of 140 °C and 120 min, initial fructose concentration of 100 g/L, catalyst load of 0.1 mg/mg.

To better clarify the structure-activity relationship of LDMC-SO_3H catalyst employed in fructose-to-5-HMF transformation, a comparison of catalytic performance of similar porous carbonaceous solid catalysts in fructose dehydration to 5-HMF with DMSO as solvent is listed in Table 2. On one hand, it is found from Table 2 that fructose conversion and 5-HMF yield obtained using catalyst carrier (LDMC) as catalyst are up to 93.8% and 34.3%, which are much higher than those (fructose conversion of 78.5% and 5-HMF yield of 8.1%) achieved in DMSO solvent without adding solid catalyst. It is proposed that besides the catalytic ability of DMSO solvent for fructose conversion discussed earlier, LDMC (catalyst carrier in this work) exerts a catalytic synergy owing to its ordered mesoporous structure for providing suitable reaction interfaces and paths (pore channels). The result confirms that as-prepared catalyst carrier in this work has certain advantages for the conver-

Table 2. Comparison in catalytic performance of similar porous carbonaceous solid catalysts in fructose dehydration to 5-HMF with DMSO as solvent

Catalyst	Reaction conditions			Catalytic performance		Structural characteristics			
	Temp. (°C)	Time (min)	Catalyst load (w/w)	X (%)	Y (%)	S_{BET} (m^2/g)	V_{meso} (cm^3/g)	D (nm)	Acidity (mmol/g)
No catalyst	140	120		78.5	8.1				
LDMC	140	120	1 : 10	93.8	34.3	260	0.075	3.42	
LDMC-SO_3H	140	120	1 : 10	100.0	98.0				
LDMC-SO_3H	130	40	1 : 2	97.2	86.7	262	0.067	3.42	0.65
LDMC-SO_3H	120	30	1 : 3	91.3	73.2				
MLC-SO_3H [18]	130	40	1 : 2	100.0	81.1	235	0.140		1.95
OMC-SO_3H [19]	120	30	1 : 3	98.7	89.4	515	0.980	7.60	1.31

sion of fructose to 5-HMF in DMSO.

On the other hand, we tried to convert fructose into 5-HMF in DMSO using LDMC-SO_3H as catalyst under the optimized reaction conditions of MLC-SO_3H derived from enzymatic hydrolysis lignin [18] and OMC-SO_3H derived from resorcinol [19], respectively. Seen from Table 2, the catalytic performance of LDMC-SO_3H in terms of 5-HMF yield (86.7%) is slightly superior to that of MLC-SO_3H (81.1%), which is probably due to the larger specific surface area and the ordered mesopores channels with suitable hydrophobic/hydrophilic balance of interfaces for the diffusion of the fructose and the produced 5-HMF in the case of much lower acid density compared to MLC-SO_3H. In the meanwhile, although the catalytic performance of OMC-SO_3H (89.4% of 5-HMF yield) is better than that of LDMC-SO_3H (73.2% of 5-HMF yield) owing to its higher specific surface area, larger ordered mesopores and higher acid density, OMC-SO_3H is synthesized using resorcinol as carbon source, which significantly increases the preparation cost and contains certain toxicity. Furthermore, under the optimized reaction conditions (reaction temperature of 140 °C, reaction time of 120 min and catalyst load of 0.1 mg/mg) obtained in this work, LDMC-SO_3H exhibits better catalytic activity (98.0% of 5-HMF yield) than MLC-SO_3H and OMC-SO_3H. The result shows that it should spend longer time on the diffusion of fructose into pore channels of LDMC-SO_3H for improving the fructose contact with its acid sites to reach the maximum values of fructose conversion and 5-HMF yield compared with MLC-SO_3H and OMC-SO_3H.

2-5. Stability of Catalyst

Besides catalytic activity, the stability of catalyst is another vital property for demonstrating its catalytic performance. To investigate the reusability of LDMC-SO_3H in DMSO, a five-cycle experiment was performed, and the result is shown in Fig. 13. Notably, 5-HMF yield is maintained at a high value of over 95.0% in five runs, highlighting that LDMC-SO_3H exerts excellent stability under the optimized reaction conditions. A slight reduction in 5-HMF yield can be attributed to the loss of sulfonic acid groups and the deposition of humins or organic residues on the LDMC-SO_3H during dehydration [32].

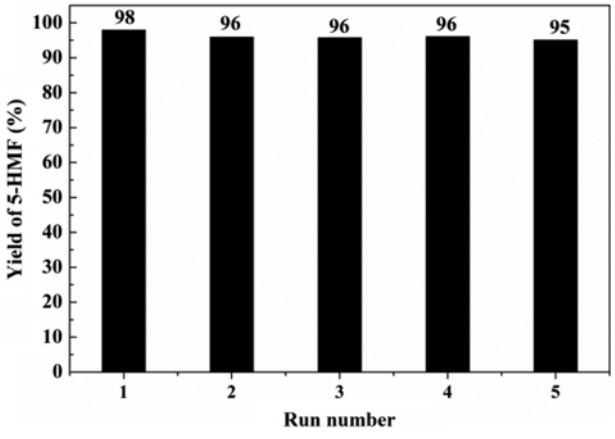

Fig. 13. Catalyst recycles for the conversion of fructose to 5-HMF. Reaction condition: reaction temperature and time of 140 °C and 120 min, initial fructose concentration of 100 g/L, catalyst load of 0.1 mg/mg, solvent of DMSO.

CONCLUSIONS

A sulfonated lignin-derived ordered mesoporous carbon was successfully prepared using kraft lignin as carbon source, and it was employed as catalyst in the dehydration reaction of fructose to 5-HMF. The single-factor experimental method was used to optimize the reaction conditions for the conversion of fructose to 5-HMF in DMSO with LDMC-SO_3H as a solid acid catalyst. The as-prepared LDMC-SO_3H had an ordered mesoporous structure with mesopore volume, specific surface area and mesopore diameter of 0.067 cm^3/g, 262 m^2/g and 3.42 nm, respectively. The sulfonic acid groups were successfully incorporated into LDMC to become the main catalytic acid sites with a density of 0.65 mmol/g. The results showed that fructose was completely converted, 5-HMF yield and reaction selectivity were both up to 98.0% under the optimized reaction conditions of 140 °C of reaction temperature, 120 min of reaction time, 100 g/L of initial fructose concentration, 0.1 mg/mg of catalyst load and pure DMSO as reaction solvent. In addition, LDMC-SO_3H exhibited excellent stability with no obvious loss of catalytic activity after five runs (5-HMF yield≥95.0%). This study not only proposes a new strategy for the value-added utilization of KL, but also provides a sustainable approach for the preparations of OMC and the acid-functionalized OMC used as solid catalyst with comparable catalytic performance for the efficient conversion of fructose to 5-HMF.

ACKNOWLEDGEMENTS

The authors are grateful for the financial support from the National Natural Science Foundation of China (grant No. 21706085) and Subsidized Project for Postgraduates' Innovative Fund in Scientific Research of Huaqiao University.

REFERENCES

1. I. K. M. Yu and D. C. W. Tsang, *Bioresour. Technol.*, **238**, 716 (2017).
2. Y. Román-Leshkov, J. N. Chheda and J. A. Dumesic, *Science*, **312**, 1933 (2006).
3. S. Zhao, M. Cheng, J. Li, J. Tian and X. Wang, *Chem. Commun.*, **47**, 2176 (2011).
4. F. S. Asghari and H. Yoshida, *Ind. Eng. Chem. Res.*, **46**, 7703 (2007).
5. J. N. Chheda, Y. Román-leshkov and J. A. Dumesic, *Green Chem.*, **9**, 342 (2007).
6. H. Hafizi, A. N. Chermahini, M. Saraji and G. Mohammadnezhad, *Chem. Eng. J.*, **294**, 380 (2016).
7. T. S. Hansen, J. Mielby, A. Riisager and A. Riisager, *Green Chem.*, **13**, 109 (2011).
8. D. M. Alonso, J. Q. Bond and J. A. Dumesic, *Green Chem.*, **12**, 1493 (2010).
9. C. Bispo, K. D. O. Vigier, M. Sardo, N. Bion, L. Mafra, P. Ferreira and F. Jérôme, *Catal. Sci. Technol.*, **4**, 2235 (2014).
10. T. S. Hansen, J. M. Woodley and A. Riisager, *Carbohydr. Res.*, **344**, 2568 (2009).
11. J. N. Chheda and J. A. Dumesic, *Catal. Today*, **123**, 59 (2007).
12. C. Antonetti, A. M. R. Galletti, S. Fulignati and D. Licursi, *Catal. Commun.*, **97**, 146 (2017).

13. J. Wang, W. Xu, J. Ren, X. Liu, G. Lu and Y. Wang, *Green Chem.*, **13**, 2678 (2011).
14. C. Tian, C. Bao, A. Binder, Z. Zhu, B. Hu, Y. Guo, B. Zhao and S. Dai, *Chem. Commun.*, **49**, 8668 (2013).
15. C. Tian, Y. Oyola, K. Nelson, S.-H. Chai, X. Zhu, J. C. Bauer, C. J. Janke, S. Brown, Y. Guo and S. Dai, *Rsc Adv.*, **3**, 21242 (2013).
16. Z. Yang, W. Qi, R. Huang, J. Fang, R. Su and Z. He, *Chem. Eng. J.*, **296**, 209 (2016).
17. F. N. D. C. Gomes, F. M. T. Mendes and M. M. V. M. Souza, *Catal. Today*, **279**, 296 (2017).
18. L. Hu, X. Tang, Z. Wu, L. Lin, J. Xu, N. Xu and B. Dai, *Chem. Eng. J.*, **263**, 299 (2015).
19. J. Wang, Z. Zhang, S. Jin and X. Shen, *Fuel*, **192**, 102 (2017).
20. J. Zhao, C. Zhou, C. He, Y. Dai, X. Jia and Y. Yang, *Catal. Today*, **264**, 123 (2016).
21. J. M. R. Gallo, R. Alamillo and J. A. Dumesic, *J. Mol. Catal. A: Chem.*, **422**, 13 (2016).
22. Y. Meng, D. Gu, F. Zhang, Y. Shi, L. Cheng, D. Feng, Z. Wu, Z. Chen, Y. Wan and A. Stein, *Chem. Mater.*, **18**, 4447 (2006).
23. S. Tanaka, N. Nishiyama, Y. Egashira and K. Ueyama, *Chem. Commun.*, **2005**, 2125 (2005).
24. S. Zhao and M. M. Abu-Omar, *ACS Sustain. Chem. Eng.*, **5**, 5059 (2017).
25. J. Podschun, B. Saake and R. Lehnen, *Eur. Polym. J.*, **67**, 1 (2015).
26. S. Yang, J.-L. Wen, T.-Q. Yuan and R.-C. Sun, *Rsc Adv.*, **4**, 57996 (2014).
27. S. Suganuma, K. Nakajima, M. Kitano, D. Yamaguchi, H. Kato, S. Hayashi and M. Hara, *J. Am. Chem. Soc.*, **130**, 12787 (2008).
28. X. Sun and Y. Li, *Angew. Chem. Int. Ed.*, **43**, 597 (2004).
29. L. Hu, G. Zhao, X. Tang, Z. Wu, J. Xu, L. Lin and S. Liu, *Bioresour. Technol.*, **148**, 501 (2013).
30. Z. Zhang, Q. Wang, H. Xie, W. Liu and Z. Zhao, *ChemSusChem.*, **4**, 131 (2011).
31. C. Guo and B. Fang, *Bioresour. Technol.*, **102**, 2635 (2011).
32. F. Guo, Z. Fang and T.-J. Zhou, *Bioresour. Technol.*, **112**, 313 (2012).
33. B. Karimi and H. M. Mirzaei, *Rsc Adv.*, **3**, 20655 (2013).
34. P. Gao, A. Wang, X. Wang and T. Zhang, *Chem. Mater.*, **20**, 1881 (2008).
35. F. Liu, C. Li, L. Ren, X. Meng, H. Zhang and F. S. Xiao, *J. Mater. Chem.*, **19**, 7921 (2009).
36. Y. Duan, F. Pan, Q Liu, Y. Zhou, A. Liang and J. Zhang, *J. Phys. Chem. C*, **121**, 1243 (2017).
37. C. Mao, J. Zhang, M. Xiao, Y. Liu and X. Zhang, *Curr. Appl. Phys.*, **18**, 1480 (2018).
38. W.-J. Liu, K. Tian, J. Hong and H. Yu, *Sci. Rep.*, **3**, 2419 (2013).
39. X. Qi, M. Watanabe, T. M. Aida and R. L. S. Jr., *Green Chem.*, **11**, 1327 (2009).
40. X. Li, K. Peng, X. Liu, Q. Xia and Y. Wang, *Chemcatchem*, **9**, 2739 (2017).
41. P. Bhanja and A. Bhaumik, *Fuel*, **185**, 432 (2016).
42. T. M. C. Hoang, E. R. H. van Eck, W. P. Bula, J. G. E. Gardeniers, L. Lefferts and K. Seshan, *Green Chem.*, **17**, 959 (2015).
43. X. Qi, M. Watanabe, T. M. Aida and R. L. S. Jr., *Green Chem.*, **10**, 799 (2008).
44. X. Qi, M. Watanabe, T. M. Aida and R. L. S. Jr., *Ind. Eng. Chem. Res.*, **47**, 9234 (2008).
45. B. F. M. Kuster, *Starch-Starke.*, **42**, 314 (2010).
46. J. Wang, J. Ren, X. Liu, G. Lu and Y. Wang, *AIChE J.*, **59**, 2558 (2013).
47. A. S. Amarasekara, L. D. Williams and C. C. Ebede, *Carbohydr. Res.*, **343**, 3021 (2008).
48. S. Hu, Z. Zhang, Y. Zhou, B. Han, H. Fan, W. Li, J. Song and Y. Xie, *Green Chem.*, **10**, 1280 (2008).
49. C. Lansalot-Matras and C. Moreau, *Catal. Commun.*, **4**, 517 (2003).
50. H. Zhao, J. E. Holladay, H. Brown and Z. Zhang, *Science*, **316**, 1597 (2007).